PREDICTION OF MAGNETIC ORIENTATION IN DRIVER GAS-ASSOCIATED −Bz EVENTS

J. Todd Hoeksema and Xuepu Zhao

Center for Space Science and Astrophysics, Stanford University
Stanford, CA 94305

To appear in JGR

Abstract

Can the magnetic orientation of driver gas in the interplanetary medium observed at Earth be predicted when its solar source is identified? Based on the exploratory assumption that the free magnetic energy present when a coronal mass ejection (CME) is initiated is transferred almost totally to other forms of energy by the time the CME stops acceleration, the potential field model can appropriately be used to calculate the magnetic orientation in the ejected plasma. As a first test of this hypothesis, we have investigated the source regions of five strong $-Bz$ events detected at 1 AU for which solar sources have been identified [Tang et al., 1989 and Tsurutani et al., 1991]. Three were traced to flare associated CMEs; one to an eruptive prominence associated CME; and one to three possible solar sources. The computed magnetic orientations at the candidate "release height" (the height where the front of a CME ceases to accelerate) above the flares sites associated with CMEs show the existence of the expected southward field component. On the other hand, the predicted field orientation at the candidate "release height" above the erupting prominence associated with a CME does not have a dominant southward field component. The result shows that the exploratory assumption may be proper only for the case of flare-CMEs. With such a severely limited number of cases, the results are only suggestive, but the magnetic orientation in flare associated CME generated driver gas may be predictable.

1. Introduction

It has long been recognized that the north-south component of the interplanetary magnetic field (IMF) in the solar-magnetospheric coordinate system plays a crucial role in determining the amount of solar wind energy transferred to Earth's magnetosphere via magnetic reconnection at the dayside magnetopause. Large southward IMF events with duration of a few hours, or $-Bz$ events, are the dominant phenomenon responsible for the development of magnetospheric substorms and the main phase of geomagnetic storms as well [Fairfield and Cahill, 1966; Tsurutani and Meng, 1972; Russell and McPherron, 1973; Gonzalez et al., 1989]. Until recently the origins of $-Bz$ events were not well understood, although several hypotheses about their origins have been presented [Gold, 1962; Akasofu, 1979; Smith, 1981; Klein and Burlaga, 1982; Gosling, et al., 1987].

Recent analysis of ISEE-3 field and plasma observations shows that the origins of the $-Bz$ events are quite varied. About half of the events detected between August 16, 1978 and December 28, 1979 occurred during the passage of the gas driving interplanetary traveling shocks [Tsurutani, et al. 1988]. It has been suggested [e.g., Kahler, 1987] that the driver gas is the interplanetary signature of the material launched in large, fast coronal mass ejections (CMEs). A model that would follow the outward transport of magnetic flux from the solar source of CMEs would be of considerable value in predicting the IMF at the Earth's orbit. However, the development of such a model is easier said than done. In fact, modeling of magnetic field transport in the interplanetary medium, at least at a level that would be useful for forecasting, is beyond the present-day state of the art (D. Swift, private communication, 1990). One naturally wonders if the orientation of the magnetic field at the origin of the CME disturbance is related to and can be used to predict the magnetic-field orientation of the driver gas [Pudovkin and Chertkov, 1976; Pudovkin and Zaitseva, 1986; Tang et al., 1985; Tang et al., 1986].

CMEs are observed by white light coronagraphs above the solar limb and are most commonly associated with eruptive prominences and solar flares accompanied by long duration soft X-ray events [e.g., Webb and Hundhausen, 1987]. The solar events associated with CMEs are usually used to pinpoint the location of the associated CMEs at the solar disk. In what follows we will use the phrase "parent event site" in reference to the position of the flare or erupting prominence supposedly associated with the CME causing a $-Bz$ event.

Based on solar wind plasma and field data from ISEE 3, Tsurutani et al. [1988, 1991] identified six driver gas-associated $-Bz$ events between 1978 and 1981, of which five were associated with solar events. In the present paper we examine these five events. By using the perpendicular to the photospheric polarity inversion line in the "flare region" to approximate the local field direction, Tang et al. [1989] found no correspondence between the magnetic orientations in driver gas-associated $-Bz$ events and those in the three corresponding flare regions. However, if the magnetic energy release in CMEs occurs at coronal altitudes [Hundhausen, 1988], the magnetic-field orientation in a driver gas-associated interplanetary $-Bz$ event may be associated with the coronal field over the parent event site, rather than the photospheric field. It is our goal here to predict the orientation of magnetic field over the parent event site based on observations of the photospheric field and to compare the prediction with interplanetary observations of $-Bz$ events. In the present paper we consider all these five events. While the number of events is limited, they serve as a first test of whether it is worth pursuing further the hypothesis that the driver gas field orientation can be predicted from the model coronal field.

2. Model and Method of Calculation

Since the magnetic field in the upper chromosphere and corona cannot currently be measured directly with useful spatial resolution, the coronal field is commonly

extrapolated from the measured photospheric fields using a potential model. The calculated potential (current-free) magnetic field is the state of minimum energy for the observed distribution of the line-of-sight component of the photospheric magnetic field [e.g., Hoeksema, 1984; Sakurai, 1985].

It is our belief that the field orientation in driver gas is more closely associated with the field orientation in CME during the "late phase" (the phase when the plasma and field of CMEs have ceased accelerating) than the "initial phase" (the phase when the plasma and field begin to accelerate). It is now widely accepted that the energy released in the CME process comes from the surplus magnetic energy, in excess of the energy of the potential field [e.g., Low, 1990]. Thus if we assume, as a exploratory hypothesis, that all the excess (or free) magnetic energy is transferred into other forms of energy before the late phase, the internal field of the CME at the late phase may be described by the potential (current-free) field model and can be inferred on the basis of observations of photospheric field.

Observations of the interplanetary disturbances may suggest how the field is configured in reality during the late phase of the CME after liberation of the excess "free" magnetic energy ends. Gosling [1990] classified the interplanetary signature of CMEs into two kinds of magnetic structures. One has large internal field rotation, like some magnetic clouds [Klein and Burlaga, 1982]. The other structure lacks large internal field rotation, like "magnetic bottles" [Gosling et al., 1987]. Nakagawa et al. [1989] identified Planar Magnetic Structures (PMS) in which all the field lines are parallel to a plane. They explained PMS as magnetic tongues and pointed out that "the magnetic field topology of a magnetic tongue is basically identical with that of the magnetic bottle". A PMS certainly has no electric current density parallel to the magnetic field; it should be a current-free field due to the divergence-free requirement on the electric current density. If a magnetic structure without large internal field rotation is associated with the magnetic structure of some CMEs (say, flare-CMEs)

at the late phase and that structure is convected to the interplanetary space by the solar wind, the magnetic structure in the associated CME must be current-free field as well. This implies that all the free magnetic energy has been transferred to kinetic and other forms of energy before the late phase of the CME and is consistent with the assumption taken here and by Sakurai [1985] in calculating the magnetic field in the flaring region. It should be noted that even though some interplanetary signatures of CMEs appear to support the assumption, the motivation of such an assumption lies not in its theoretical implications but in seeing whether positive results may be obtained using the hypothesis that the field orientation of some driver gas can be predicted from the model coronal field. We will discuss the validity of this assumption further later in the paper .

The solar wind outflow significantly affects the coronal magnetic field configuration. Source surface models can be used to mimic the most important effects of the solar wind and they provide a credible approximation to the full MHD solution of Pneuman and Kopp [1971] in the region below the source surface [Wolfson, 1985 and references therein]. While high resolution mapping of the current-free coronal magnetic field above limited photospheric regions is possible with the Schmidt [1964] and other related programs [e.g., Sakurai, 1985], such methods suffer from the need for specification of boundary conditions at the edges of a limited photospheric region. These boundary conditions are equivalent to assumptions about how neighboring photospheric regions contribute to the coronal magnetic field being calculated.

Here we model the orientation of the coronal field above a parent event site including the effects of solar wind outflow and neighboring regions. We use the source surface potential field code with the source surface located at 2.5 $R_{\odot}$ [Hoelsema et al., 1982,3; Hoeksema, 1984]. The predicted source surface field direction matches the daily IMF polarity about 80% of the time with a fixed time lag of 4.5 days.

The inner boundary condition is the synoptic chart of the line-of-sight photo-

spheric magnetic field. The maps are assembled from magnetograms collected over a complete solar rotation which emphasize central meridian observations. Accordingly the photospheric data were generally not taken at the time of the event. To obtain the required spatial resolution we compute the spherical harmonic expansion of National Solar Observatory (NSO) magnetic fields observations to spherical harmonic order 42. This truncation limit is used because it corresponds to the resolution of the averaged data and because the method of constructing synoptic charts filters out higher spatial frequencies [Altschuler et al. 1977]. Because the source surface calculation is a global one, distortions introduced at the edges of the data window, where the fields are observed about 27 days apart, must be minimized by locating the region of interest at the center of the computational window. The contour map in Figure 1 shows the photospheric line-of-sight magnetic field over the entire Sun. A small circle shows the location of a flare that occurred at E31° S25° on March 30, 1979, 21:13 UT. Tang et al. [1989] associated this flare with the coronal mass ejection that produced the driver gas which caused the $-Bz$ event observed near Earth by ISEE-3 on April 3, 1979.

It should be emphasized that the north and south directions in the chart are defined with respect to the solar equator, but the north-south direction of the IMF is taken in the Geocentric Solar Magnetospheric (GSM) system. To carry out the transformation between the two coordinate systems, we calculate the position angle of the northern extremity of the Earth's rotation axis (NERA) at the time of the parent event, which is, on a one-day average, parallel to the projection of Z-axis of the GSM coordinate system onto the Carrington coordinate system. The mark on the circle centered at the parent event site denotes the direction of the Earth's rotation axis during this event. With this additional correction, the method of Tang et al. [1989] gives the magnetic orientation of the parent event at the photosphere, 1 $R_{\odot}$, as eastward (E, in Table 1) with respect to the Earth's rotation axis.

As discussed above, the driver gas creating the interplanetary shock approaches a constant velocity in the late phase of the CME. For convenience we will call the height where the front of CMEs ceases to accelerate the "release height". Since we assume the magnetic configuration at the "release height" is closely related to the magnetic configuration in the driver gas, the calculations are executed for specified candidate heights. HAO's K-coronameter observations show that flare-associated events exhibit little acceleration in the height range 1.2–2.4 $R_\odot$, while eruptive prominence-associated events experience great acceleration [MacQueen and Fisher, 1983]. In other words, the release height of flare associated events is below the height limit of routine coronal observations, but is close to or higher than the usual source surface radius for eruptive prominence-CMEs. The above classification of CMEs remains an open question [Webb and Hundhausen, 1987; Wagner, 1988] and will be discussed later in the paper.

Recently Wagner [1988] identified incipient CMEs with eruptive prominence- and flare-associated 5303Å emission line transients. These green line events appear to be initiated below 25000 km in the corona, implying that CMEs are probably initiated below 1.035 $R_\odot$. We therefore select $1.03R_\odot$ and 1.20 $R_\odot$ (the lower limit of routine coronal observations) as representative release heights for flare-associated CMEs and $2.49R_\odot$ (the height just below the source surface) for eruptive prominence-associated CMEs. It should be noted that the acceleration of the fast flare-CMEs might not be measured adequately with the present height/time data [Webb, private communication, 1991], the release heights estimated here are only suggestive. To see the effect of the "release height" on the prediction of magnetic orientation, we calculate the magnetic orientation at all three heights for each event.

Figure 2 shows the field direction at $1.03R_\odot$ computed from the photospheric field displayed in Figure 1. The '+' symbols mark grid points having a radial field component out of the Sun, 'x' symbols indicated field into the Sun. The contour of

zero radial field is drawn on the chart. The arrow drawn from each grid point shows the direction of the transverse field computed from the θ and ϕ components. This plot gives no indication of the magnitude of the field.

The field has a southward component at $1.03R_{\odot}$ at the parent event site. The transverse field is directed south-east (SE) with respect to the Earth's rotation axis, consistent with the observed magnetic orientation in the $-$Bz event (See Table 1). Figures 3 and 4 show the the predicted field direction at $1.20R_{\odot}$ and $2.49R_{\odot}$, respectively.

3. Prediction and Comparison

Using a full complement of solar wind plasma and magnetic field data from ISEE-3 in the interval 1978–1979, Tsurutani et al. [1988] identified four $-$Bz events associated with driver gas. These events, having Bz < -10 nT and duration > 3 hours, were responsible for intense geomagnetic storms with Dst < -100 nT. The solar source of three of these events were flares or erupting prominences associated with CMEs [Tang et al., 1989]. Recently Tsurutani et al. [1991] identified two more driver gas-associated $-$Bz events in 1980–1981 which generated superstorms with Dst ≤ -250 nT and were clearly related to identifiable solar flares or erupting prominences. The magnetic field orientation at the location of the candidate parent events for each of the five $-$Bz events at the altitudes $1.03R_{\odot}$, $1.20R_{\odot}$, $2.49R_{\odot}$, and $1.0R_{\odot}$ are shown in Table 1.

The first and second columns of Table 1 list the times at which the gas driving interplanetary shocks and the $-$Bz events were observed. The magnetic orientation in GSM coordinates of the observed $-$Bz events is shown in parentheses in the second column. The next columns identify the candidate solar sources of the $-$Bz events, the relative orientation of the Sun's and Earth's rotation axes, and the predicted magnetic orientations at various altitudes. The coordinates of the erupting prominences in

Table 1 are for the "center" point of the preexisting quiet prominences; however, prominences are often quite extended in length [F. Tang, private communication, 1991]. The magnetic orientations at $1.0R_{\odot}$ in Table 1 are obtained by using a method similar to Tang et al. [1989], but here the orientation is relative to the Earth's rotation axis, rather than the Sun's. We assigned each event to one of eight 45 degree sectors, N, NW, etc. relative to the Earth's rotation axis. For instance, the orientation of E at $1R_{\odot}$ for the 30 March, 1979 event (see Table 1), indicates a transverse field direction between 247.5° and 292.5°. The actually measured angle is 270.0° (corresponding to 245.0° relative to the Sun's rotation axis). We inferred the magnetic orientation at $1R_{\odot}$ from NSO, rather than WSO, magnetic observations, which may be the reason why our inference for the 30 March, 1979 event is not consistent with that of Tang et al (see Figure 1).

The first three −Bz events are associated with only one candidate parent event. The fourth −Bz event has four candidate flares, but fortunately all four flares are located within the same active region [Tsurutani, private communication, 1991].

The fifth event has three widely separated candidate parent events. The prediction for the first candidate flare shows the existence of the southward component, but the second candidate flare and the erupting prominence show no southward component. The observed velocity marginally favors identifying the first event as the source, but the uncertainty in velocity is too great to eliminate any of the solar events. Since we cannot be sure which source led to the interplanetary driver gas and the −Bz event, we can infer nothing from this event.

Of the other four −Bz event sources, one is an erupting prominence CME and three are flare CMEs. The predicted magnetic orientations have a dominant southward field component at none of the selected coronal altitudes for the erupting prominence event. However, the orientations over all three flare associated events have a southward component at both 1.03 and 1.20 $R_{\odot}$; only one of the events has a southward component

at 2.49 $R_\odot$.

4. Discussion

On the basis of the exploratory assumption that the free magnetic energy in the CME source region is totally transfered to other forms of energy before the late phase, we use the potential field code to predict the magnetic orientation above the solar sources of driver gas-associated $-$Bz events. To see if the results are correct we compare the predicted results with the in situ observations of the associated $-$Bz events. For this very limited set of four 'clear' events, the method predicts the existence of a southward field component both at 1.03 and 1.20 $R_\odot$ for the three flare CMEs and the absence of a southward component at 2.49 $R_\odot$ for the one erupting prominence CME. Three of four events do not have a southward component at heights which are not the supposed "release height." The results suggest that separation into flare-CME and eruptive prominence-CME classes may be required for prediction of magnetic orientation of the driver gas-associated $-$Bz events because the assumption of total release of free magnetic energy during the late phase of CMEs may not be proper for the case of eruptive prominence-CMEs. Distinguishing characteristics of flare-CMEs and eruptive prominence-CMEs have been detected at both coronal altitude [MacQueen and Fisher, 1983] and near the Earth's orbit [Wright, 1990; Gosling, 1990]. Observations and theory have shown that neither flares nor eruptive prominences appear to drive CMEs, leading to the eventual recognition that mass ejections are coronal eruptions in their own right. Our understanding of CME initiation and propagation has progressed greatly, especially for the eruptive prominence-CMEs [Hundhausen, 1988; Low, 1990]. The existence of the three part structure in the eruptive prominence-CMEs shows that the internal field of eruptive prominence-CMEs is certainly not potential, which is further supported by the fact that many magnetic clouds can be approximately described by the force-free field model and associated with eruptive

prominence-CMEs [Marubashi, 1986]. That may be why the assumption made in the present work is proper only for the case of flare-CMEs and the model developed here may only be used to predict the magnetic-field orientation of driver gases associated with flare-CMEs. Generally speaking, the CME magnetic field is the sum of the potential field due to the presence of external electric currents lying below the photosphere and above the "source surface" plus the field contributed by whatever internal electric currents the CME possesses. It is not appropriate, in general, to expect the potential model to accurately describe the internal field of CMEs. Even for the case of flare-CME, the assumption made here must be oversimplification. Caution must be excercised in making any theoretical inferences from this model.

The classification into eruptive prominence-CMEs and flare-CMEs remains an open question, as mentioned in the first section of the paper. CMEs originate in closed magnetic regions of the solar atmosphere. The SMM coronagraph observations in the ascending phase of Cycle 21 further showed [NCAR High Altitude Observatory Report, 1991] that CMEs related to the eruption of major quiescent prominences at high latitudes form a distinct class. The erupted prominence tends to show a characteristic ropelike structure. These events sometimes occur without X-ray or H_α emissions that would be classified as flares. A second distinct class of CMEs is associated with observed eruptions of chromospheric material from active regions. These occur in low or middle latitudes and are characterized by amorphous or complex dense cores, many examples associated with X-ray and H_α flares. Perhaps CMEs would better be classified as quiescent prominence-CMEs and active region-CMEs instead of as eruptive prominence-CMEs and flare-CMEs, respectively [David Sime, private communication, 1991].

The consistency between the in situ observations of magnetic orientation in driver gas-associated $-Bz$ events and the prediction at the "release heights" of flare-CMEs implies that the field is probably convected from the corona to the Earth's orbit.

Marubashi [1986] also inferred that many magnetic clouds are extended or propagated through corona[1] and interplanetary space with their configuration almost unchanged.

Harrison [1986] found that flare-associated CMEs appeared to leave the solar surface during weak soft X-ray bursts preceding subsequent associated flares by tens of minutes. The precursor X-ray brightenings had a large spatial scale size, $\sim 10^5$ km, and the resulting flares were positioned near one leg of the angle subtended by the CME. Harrison's scenario places the sources of flare-associated CMEs in large X-ray arches connecting different active regions. The magnetic fields in these arches may be close to potential, as assumed here. However, the flare cannot be the site of the CME because flares sit well to one side of of the center line of the CMEs. To search for the dominant polarity in the area covered by the soft X-ray bursts, we drew a thick 10^5 km radius semicircle centered at the parent event site extending across the polarity inversion line (see Figures 1, 2 and 3), and found that a dominant southward component exists in the thick semicircle for the event analyzed. However, it is usually difficult to determine the position of a flare with respect to the polarity inversion line because flares are typically located very close to contorted inversion lines.

Roughly 10–30% of the interplanetary counterparts of CMEs include signatures of magnetic clouds [Gosling, 1990]. The magnetic configuration of magnetic clouds can be approximately described by a constant α force-free field model [Burlaga, 1988]. It would be interesting to investigate the magnetic orientation in the source region using a force-free field model. Unfortunately, we cannot carry out the calculation because the available line-of-sight photospheric data for the events studied here provide no information on the electric current. For the events considered here the vector magnetic field required to do force-free model calculations are not available.

While the limited number of events makes any conclusions tenuous at best, the success in predicting the field orientation is tantalizing and encourages a continued investigation with a larger sample of events.

Acknowledgement.

We thank P. Scherrer, B. Tsurutani and F. Tang for helpful discussions, J. Klimchuk, P. Milford and D. Webb for reading and commenting on the manuscript, J. Harvey for providing data from the National Solar Observatory and B. Tsurutani and F. Tang for providing two driver gas-associated $-$Bz events in 1980-1981 before their publication. This work was supported in part by the Office of Naval Research under Grant N00014-89-J-1024, by the National Aeronautics and Space Administration under Grant NGR5-020-559, and by the Atmospheric Sciences Section of the National Science Foundation under Grant ATM90-22249.

REFERENCES

Akasofu, S.-I., Energy coupling between the solar wind and the magnetosphere, *Space Sci. Rev., 28*, 121–190, 1981.

Altschuler, M. D., R. H. Levine, M. Stix and J. Harvey, High resolution mapping of the magnetic field of the solar corona, *Solar Physics, 51*, 345–375, 1977.

Burlaga, L. F., Magnetic clouds and force-free fields with constant Alpha, *J. Geophys. Res., 93*, 7217–7224, 1988.

Fairfield, D. H. and L. J. Cahill, Transition region magnetic field and polar magnetic disturbances, *J. Geophys. Res., 71*, 155–169, 1966.

Gold, T., Magnetic storms, *Space Sci. Rev., 1*, 100–164, 1962.

Gonzalez, W. D., B. T. Tsurutani, A. L. C. Gonzalez, E. J. Smith, F. Tang, and S.-I. Akasofu, Solar wind-magnetosphere coupling during intense magnetic storms, *J. Geophys. Res., 94*, 8835–8851, 1989.

Gosling,J. T. and D. J. McComas, Field line draping about fast coronal mass ejecta: A source of strong out-of-the-ecliptic interplanetary magnetic fields, *Geophys. Res. Lett., 14*, 355–358, 1987.

Gosling, J. T., Coronal mass ejections and magnetic flux ropes in interplanetary space, in *Physics of Magnetic Flux Ropes* ed. by C. T. Russell, E. R. Priest, L. C. Lee, pp. 343–364, American Geophysical Union, Washington DC, 1990.

Harrison, R. A., and G. M. Simnett, Soft X-ray bursts associated with coronal mass ejection onset, in *STIP Symposium on Retrospective Analyses*, edited by M. A. Shea and D. F. Smart, Book Crafters, Chelsea, Michigan, 1986.

High Altitude Observatory, *Bulletin American Astronomical Society, 23*, 453–465, 1991.

Hoeksema, J. T., Structure and Evolution of the Large Scale Solar and Heliospheric Magnetic Fields, thesis, Stanford University, CSSA-ASTRO-84-07, 1984.

Hoeksema, J. T., J. M. Wilcox. and P. H. Scherrer, Structure of the heliospheric current sheet in the early portion of sunspot cycle 21, *J. Geophys. Res., 87*, 10331–10341, 1982.

Hoeksema, J. T., J. M. Wilcox, and P. H. Scherrer, Structure of the heliospheric current sheet: 1978–1982, *J. Geophys. Res., 88*, 9910–9920, 1983.

Hundhausen, A. J., The origin and propagation of coronal mass ejections, in *Proceeding of the Sixth International Solar Wind conference*, edited by V. Pizzo, T. E. Holzer, and D. G. Sime, NCAR/TN-306+Proc, Boulder, Colo., p. 181, 1988.

Kahler, S., Coronal mass ejections, *Rev. Geophys., 25*, 663–675, 1987.

Klein, L. W., and L. F. Burlaga, Interplanetary magnetic clouds at 1 AU, *J. Geophys. Res., 87*, 613–624, 1982.

Low, B. C., Equilibrium and dynamics of coronal magnetic fields, *Annu. Rev. Astron. Astrophys. 28*, 491–524, 1990.

MacQueen, R. M., and R. R. Fisher, The kinematics of solar inner coronal transients, *Solar Phys., 89*, 89–102, 1983.

Marubashi, M., Interplanetary magnetic clouds and solar filaments, *Adv. Space Res., 6*, 335–344, 1986.

Nakagawa, T., A. Nishida and T. Saito, Planar magnetic structures in the solar wind, *J. Geophys. Res., 94*, 11,761–11,775, 1989.

Pneuman, G.W., and Kopp, Gas-magnetic field interactions in the solar corona, *Solar Phys., 18*, 258–270, 1971.

Pudovkin, M. I., and A. D. Chertkov, Magnetic field of the solar wind, *Solar Phys., 50*, 213–229, 1976.

Pudovkin, M. I. and S. A. Zaitseva, Comment on "Magnetic field on the sun and the north-south component of transient variation of the interplanetary magnetic field at 1 AU by F. Tang et al., *J. Geophys. Res., 91*, 11,765–11,768, 1986.

Russell, C. T., and R. L. McPherron, The magnetotail and substorms, *Space Sci. Rev., 15*, 205–266, 1973.

Sakurai, T., Magnetic field structures of hard X-ray flares observed by Hinotori spacecraft, *Solar Phys., 95*, 311–321, 1985.

Smith, E. J., Solar wind magnetic field observations, Solar Wind Four, *Tech. Rep. MPAE-W-100-81-31*, edited by H. Rosenbauer, p. 96, Max-Planck-Institut fur Aeronomie, Katlenburg-Lindau, Federal Republic of Germany, 1981.

Tang, F., S.-I. Akasofu, E. Smith and B. Tsurutani, Magnetic field on the sun and the north-south component of transient variation of the interplanetary magnetic field at 1 AU, *J. Geophys. Res., 90*, 2703–2712, 1985.

Tang, F., S.-I. Akasofu, E. Smith and B. Tsurutani, Reply, *J. Geophys. Res., 91*, 13,769–13,769, 1986.

Tang, F., B. T. Tsurutani, W. D. Gonzalez, S.-I. Akasofu, and E. J. Smith, Solar source of interplanetary southward Bz events responsible for major magnetic storms (1978–1979), *J. Geophys. Res., 94*, 3535–3541, 1989.

Tsurutani, B. T. and C.-I. Meng, Interplanetary magnetic-field variations and substorm activity, *J. Geophys. Res., 77*, 2964–2970, 1972.

Tsurutani, B. T., W. D. Gonzalez, F. Tang, S.-I. Akasofu, and E. J. smith, Origin of interplanetary southward magnetic field responsible for major magnetic storms near solar maximum (1978–1979), *J. Geophys. Res., 93*, 8519–8531, 1988.

Tsurutani, B. T., W. D. Gonzalez, F. Tang, and Yen Te Lee, Great magnetic storms, *Geophys. Res. Lett.*, in press, 1992.

Wagner, W. J., Understanding the structure and dynamics of the inner corona through emission line transients and coronal mass ejections, in *Solar and Stellar Coronal Structure and Dynamics*, edited by R. C. Altrock, National Solar Observatory / Sacramento Peak, Sunspot, pp. 473–500, 1988.

Webb, D. F. and A. J. Hundhausen, Activity associated with the solar origin of coronal mass ejections, *Solar Phys., 108*, 383–402, 1987.

Wolfson, R., A coronal magnetic field model with volume and sheet currents, *Astrophys. J., 288*, 769–778, 1985.

Wright, C., A comparison of the signatures of disappearing filaments and flares in the interplanetary medium at 1 AU, and their relationships to geomagnetic disturbances, *Solar-Terrestrial Predictions: Proceedings of a workshop at Leura, Australia, October 16-20, 1989, Volume 1*, ed. by R. J. Thompson et al., NOAA, Boulder, 658–663, 1990.

Captions

Figure 1. The NSO synoptic chart of the photospheric magnetic field with the 1979/03/30 21:13 UT (N27 W19) flare-associated CME centered. The field has been averaged into 30 bins of sine latitude from north to south each 5 Carrington degrees. The photosphere is shown in an equal area projection (equal steps in sine latitude). The bottom axis shows the Carrington longitude, while the top axis is labeled by central meridian passage date. The small circle denotes the location of the flare associated with a CME and $-$Bz event. The thick arrow denotes the orientation of Earth's rotation axis when the flare occurred.

Figure 2. Predicted the magnetic orientation at 1.03 $R_{\odot}$. The small circle and the thick arrow have the same meaning as in Figure 1.

Figure 3. Predicted the magnetic orientation at 1.20 $R_{\odot}$. The small circle and the thick arrow have the same meaning as in Figure 1.

Figure 4. Predicted the magnetic orientation at 2.49 $R_{\odot}$. The small circle and the thick arrow have the same meaning as in Figure 1.

Table 1: Comparison Between Observation and Prediction

Driver Gas UT	−Bz Event UT	Solar Source UT Location	NERA	Field Orientation 1.0	1.03	1.20	2.49
1978/08/27 18:00	1978/08/27 20:00 (SE/SW)	1978/08/23 01:14,12:00 N15 E15 Prom Erup	19°	NW	NW	NW	N
1978/09/29 08:13	1978/09/29 08:13 (SW)	1978/09/27 14:28 N27 W19 Flare	25°	E	S	S	E
1979/04/03 19:30	1979/04/03 19:30 (SE)	1979/03/30 21:13 S25 E31 Flare	-26°	E	SE	SE	S
1980/12/19 13:00	1980/12/19 12:00 (SE/SW)	1980/12/16 09:59 N06 E24 Flare 11:54 N12 E20 Flare 14:54 N09 E14 Flare 1980/12/17 12:09 N10 E07 Flare	9°	E	SE	SE	N
1981/04/13	1981/04/12 23:00 (SW/SE)	1981/04/10 12:25 N11 E53 Flare	-26°	W	SW	SW	NE
		16:55 N08 W38 Flare		E	NE	N	N
		20:00 N00 E38 Prom Erup		NE/E	E	E	E

nsosynop synop.field   1/16/92 0, ±300, 600, 1500, 3000, 6000 MicroTesla

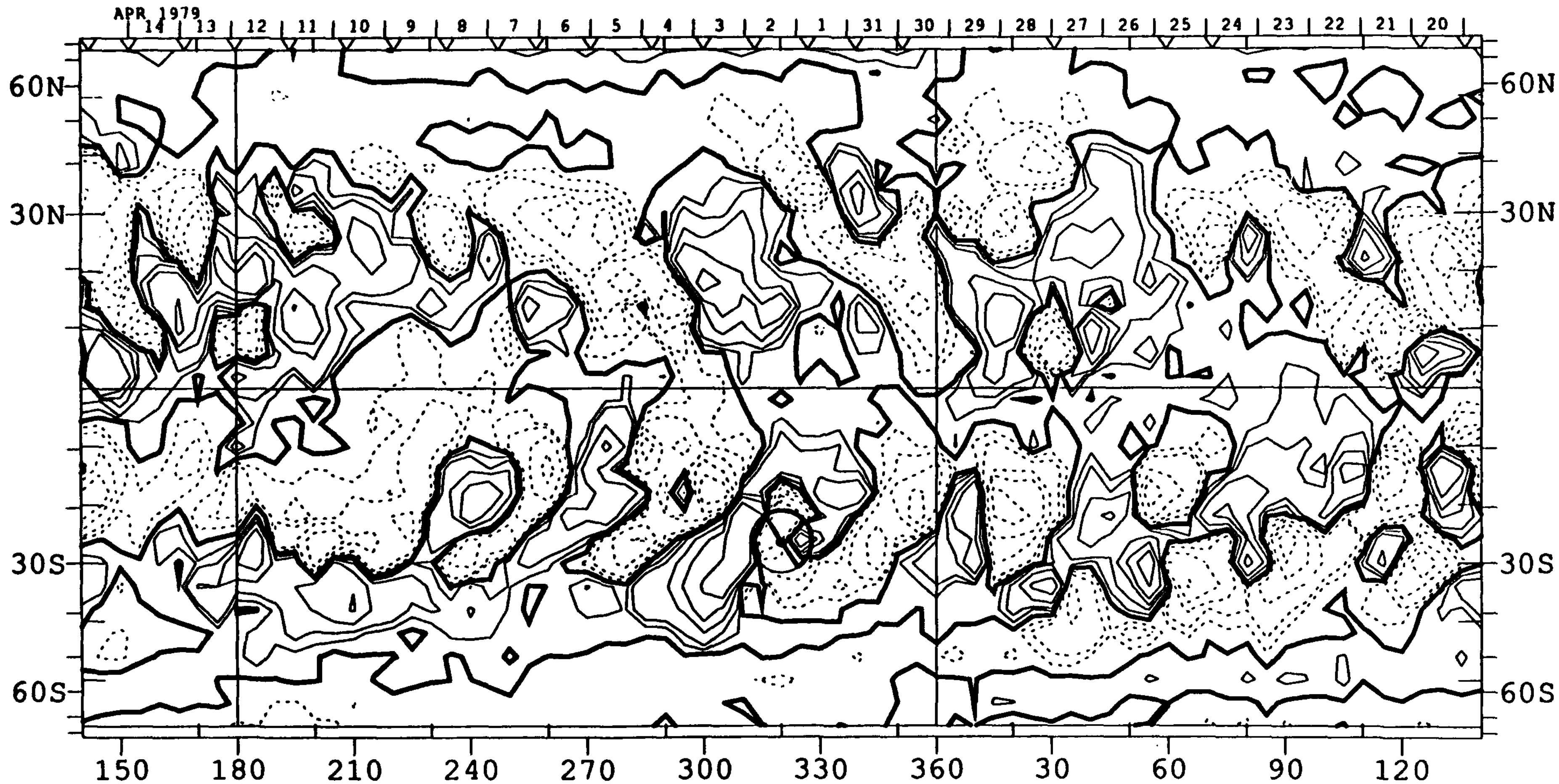

1680

arrowplot by zhao at 1992:01:16_12h:18m:40s
$ dsph5 in=nsosynop frot=1680 center=ct1680:320 mono=1 order=42 r=1.03

Rs @ 2.5

Direction of magnetic field at r=1.03   2 APR 1979

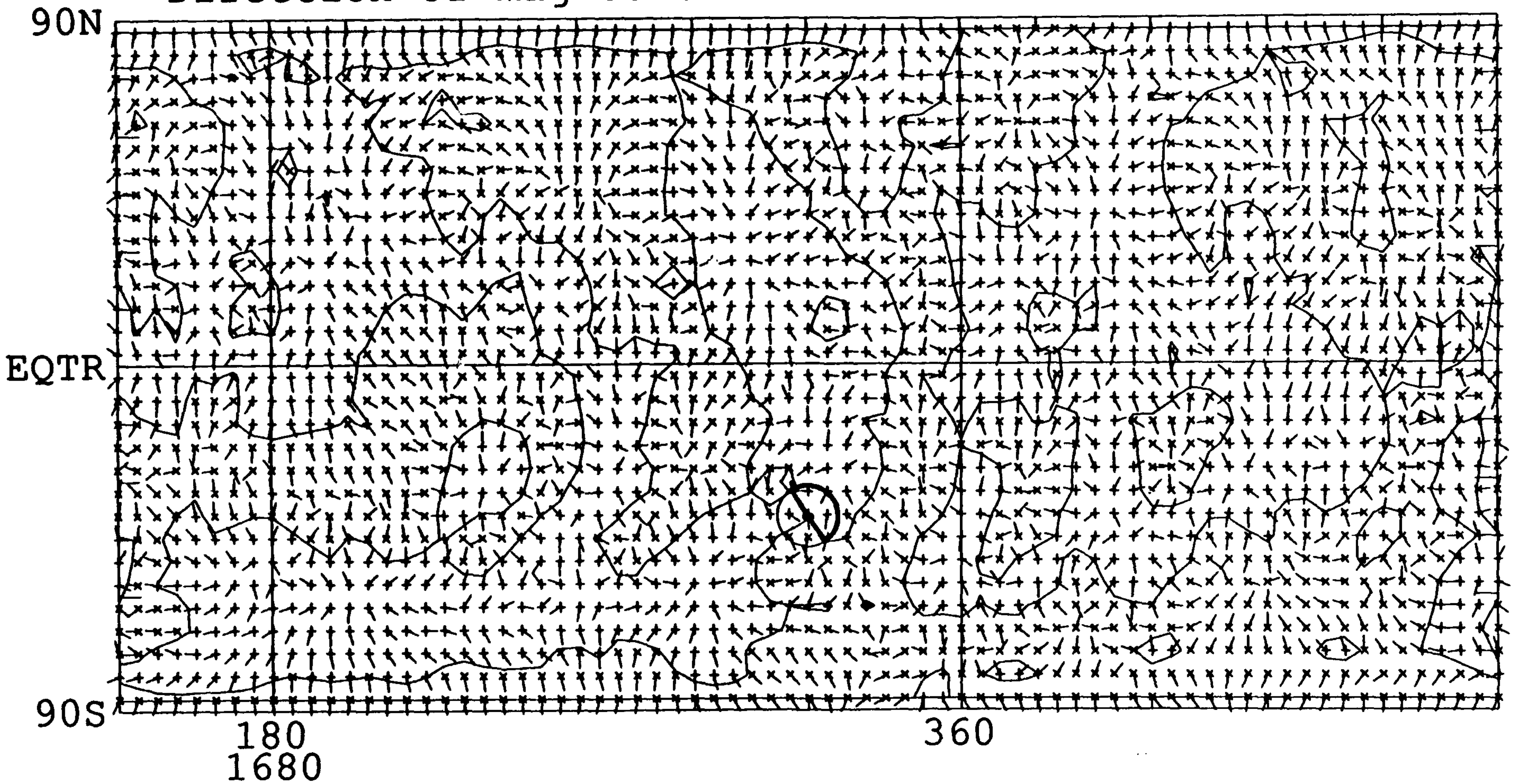

arrowplot by zhao at 1992:01:16_12h:19m:44s
$ dsph5 in=nsosynop frot=1680 center=ct1680:320 mono=1 order=42 r=1.20

Rs @ 2.5

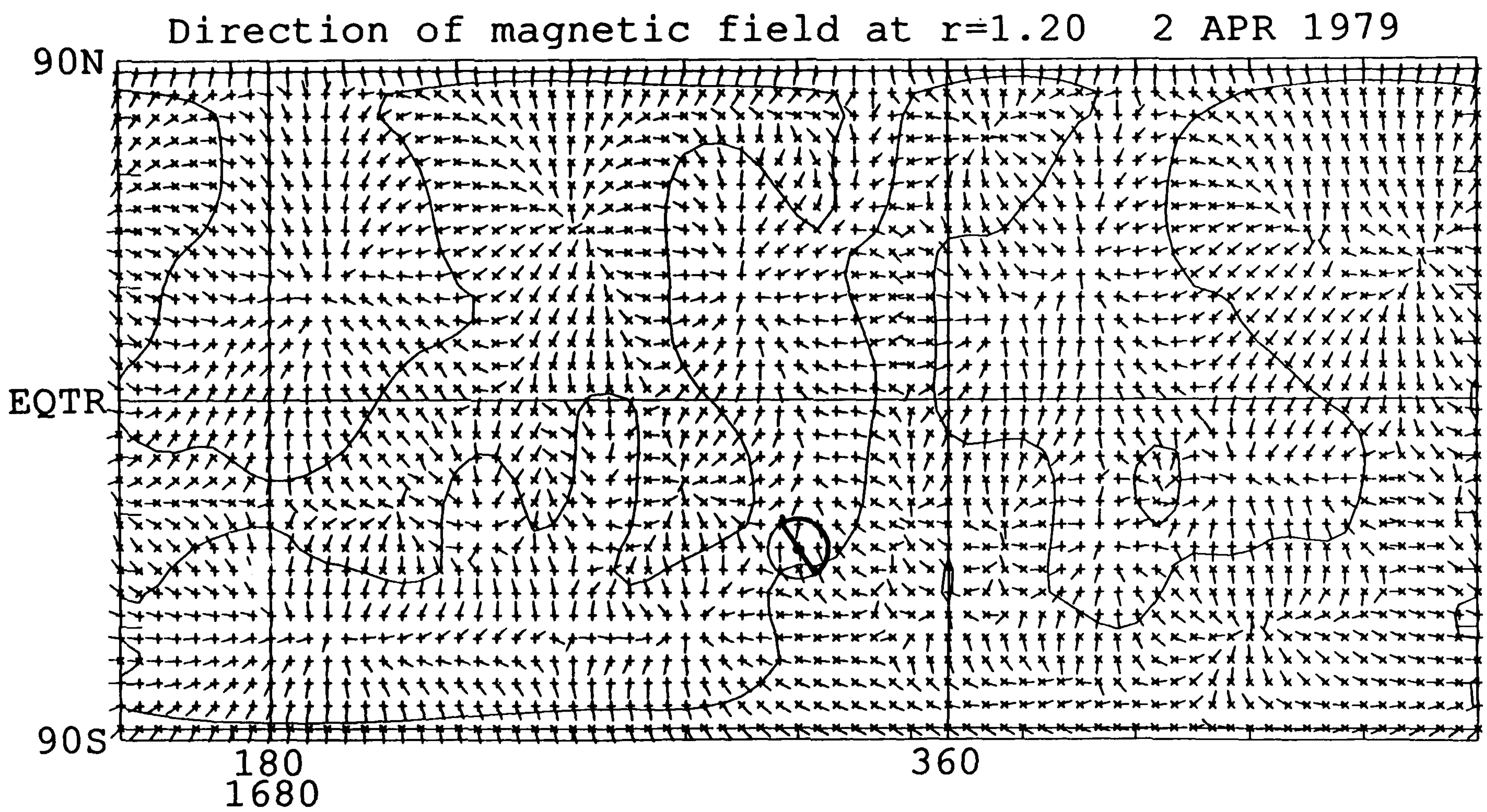

arrowplot by zhao at 1992:01:16_12h:20m:20s
$ dsph5 in=nsosynop frot=1680 center=ct1680:320 mono=1 order=42 r=2.49

Rs @ 2.5

Direction of magnetic field at r=2.49   2 APR 1979